

## STM studies of the effect of pretreatment on the morphology and aspect ratio distribution of crystallites on Pt/HOPG

King Lun Yeung and E.E. Wolf \*

*Department of Chemical Engineering, University of Notre Dame, Notre Dame, IN 46556, U.S.A.*

STM studies of chemically impregnated model Pt catalysts supported on HOPG substrate reveal the dynamics of morphological transformation from catalyst-intermediate to metal crystallites of near-equilibrium shape. Both the morphology and aspect ratio distribution of the crystallites undergo significant changes for catalysts reduced for 0.5, 2, and 60 h at similar pretreatment conditions. The aspect ratio distribution shows that majority (60–70%) of the crystallites have metastable shapes. Another model Pt catalyst was prepared by vacuum deposition of Pt metals onto the graphite substrate. Prior to H<sub>2</sub> pretreatment, the Pt particles have random, irregular morphologies which transform to regular spherical shapes after H<sub>2</sub> treatment at 250°C for 30 min.

**Keywords:** STM; Pt/graphite; pretreatment effect

### 1. Introduction

Recent years have seen significant progress in the application of scanning tunneling microscopy (STM) in the characterization of the microstructure of surfaces [1–10] and the morphologies of small clusters [11–14]. Earlier studies concentrated on well ordered, single crystal surfaces of semiconductors [1–3] and metals [4–10], but recent studies extend toward quasicrystals [15] and small semiconductor and metal clusters [11–18]. While in principle STM can help in elucidating the phenomenological effect of catalyst microstructures, there are only few STM applications devoted to the study of supported catalyst particles [15–18].

The objective of this STM work is to study model Pt supported catalysts prepared under conditions that are similar to that used in typical catalyst preparation. Such method involves deposition of the catalyst precursor onto

\* To whom correspondence must be addressed.

support materials from a liquid solution with subsequent treatment in both oxidizing and reducing atmospheres to convert the catalyst-intermediates to its active metallic form. While in general the metal catalysts are usually supported on porous oxides, due to the requirement of the STM technique, we selected graphite as the catalyst support. In this paper, the effect of reduction time on the catalyst size and morphology was studied to determine the dynamics of morphological transformation from catalyst-intermediates to reduced metal crystallites of near-equilibrium morphology.

## 2. Experimental

### CATALYSTS PREPARATION AND PRETREATMENT

The Pt catalysts were prepared by depositing 40  $\mu\text{l}$  of 0.108 M solution of chloroplatinic acid in a 1.0 M HCl on a freshly cleaved surface of a highly oriented pyrolytic graphite or HOPG (ZYH Grade, UCAR Carbon Company Inc.). A thin, uniform film of liquid solution was obtained by first dispersing micro-droplets of the solution on the graphite surface, then the liquid was pressed between two graphites layers. The amount of solution used is critical to both the thickness and the integrity of the film. Too much solution results in a thick liquid film while too little causes the film to break up into patches. The deposition was conducted at room temperature for 12 h. The resultant supported precursors were dried at 373 K in air for 24 h. The dried catalysts were then decomposed in flowing Ar (UHP, Linde Union Carbide) at 873 K for 2 h, reduced in flowing  $\text{H}_2$  (UHP, Linde Union Carbide) at 723 K for 0.5, 2, and 60 h respectively, and finally outgassed at 673 K in flowing Ar for another 2 h. The catalysts were then slowly cooled back to room temperature in Ar.

A second model catalyst was also prepared by evaporating 15.7 mg ( $\sim 10$  Å film thickness) of Pt foils (99.999% Pt, Engelhard Corp.) at  $1 \times 10^{-6}$  Torr onto nuclear grade high purity graphite (NGHPG). The model catalyst was then treated in  $\text{H}_2$  at 523 K for 30 min, then heated rapidly from 523 to 773 K (8 min duration) and finally cooled back to room temperature in flowing Ar.

### STM CHARACTERIZATION

The STM used in this study is a commercial Nanoscope II (Digital Instrument Inc.) operated in ambient conditions. Two STM heads of different scan range were employed, a short scan head of 500 nm range and a medium scan head of 7500 nm range. The STM was operated in the height imaging mode with the operational bias voltage kept between 50 and 150 mV and the tunneling current at 1 nA. The horizontal scan frequency was maintained below 26 Hz.

### 3. Results and discussion

#### MORPHOLOGIES OF Pt SUPPORTED CATALYSTS

The images of highly oriented pyrolytic graphite (HOPG) have been presented previously [18], since HOPG serves as a standard for STM calibration and its surface structure has been well studied. The typical surface of HOPG is very flat and microscopically smooth, consisting primarily of large terraces separated by occasional monoatomic steps. Atomic resolution images of the HOPG surface usually show a hexagonal close packed arrangements of the graphite structure with a measured nearest neighbor distance of  $\sim 2.3$  Å. Whereas the well ordered surface of the HOPG substrate makes it an ideal support for STM studies, the surface is also lubricating which sometimes results in the displacement of the deposited materials [19,20] by the rastering tip of the STM.

After partial decomposition of the deposited precursors in Ar, the catalysts were reduced in  $H_2$  at 723 K for different length of time to study the effect of the reduction time on the morphology and size of the catalyst particles. Both separately reduced and sequentially reduced catalyst samples were studied. In the sequentially reduced sample, the catalyst was taken out at various time intervals for STM characterization which entails repeated exposure to air. The morphologies of the crystallites in both types of samples are very similar, therefore, only the results for separately reduced samples are presented.

It is relevant to note that about 300–400 crystallites were imaged and measured in each sample for the purpose of obtaining statistically significant data, with the exception of the model catalyst prepared from vacuum deposition of Pt metal in which only about 100 crystallites were measured. The images shown below were selected to be representative of the crystallite morphology of each sample, however the conclusions were based on the statistical measurements obtained from each sample rather than on the individual images shown.

*a). 0.50 hour* The morphologies of the Pt particles after half an hour of reduction are shown in fig. 1, with fig. 1a showing both large elongated particles and aggregates of smaller, oblong crystallites. The rod-like particles tend to bundle together and seems to be originally part of a larger particle. Fig. 1b shows small crystallites aggregated in well ordered manner with 4–5 crystallites oriented in a straight line. The arrangement of these crystallites indicates an original elongated morphology, similar to the rod-like particles shown in fig. 1a. In fact fig. 1b shows some of the rod-like particles at various stages of decomposition into smaller particles. The variety of morphologies and the well ordered arrangement of the particles are indicative that we are observing an intermediate step of the decomposition process from catalyst intermediates into metallic crystallites. The results shows that an originally large particle (fig. 1a) develops striation marks along its surface upon exposure to  $H_2$ , and eventually

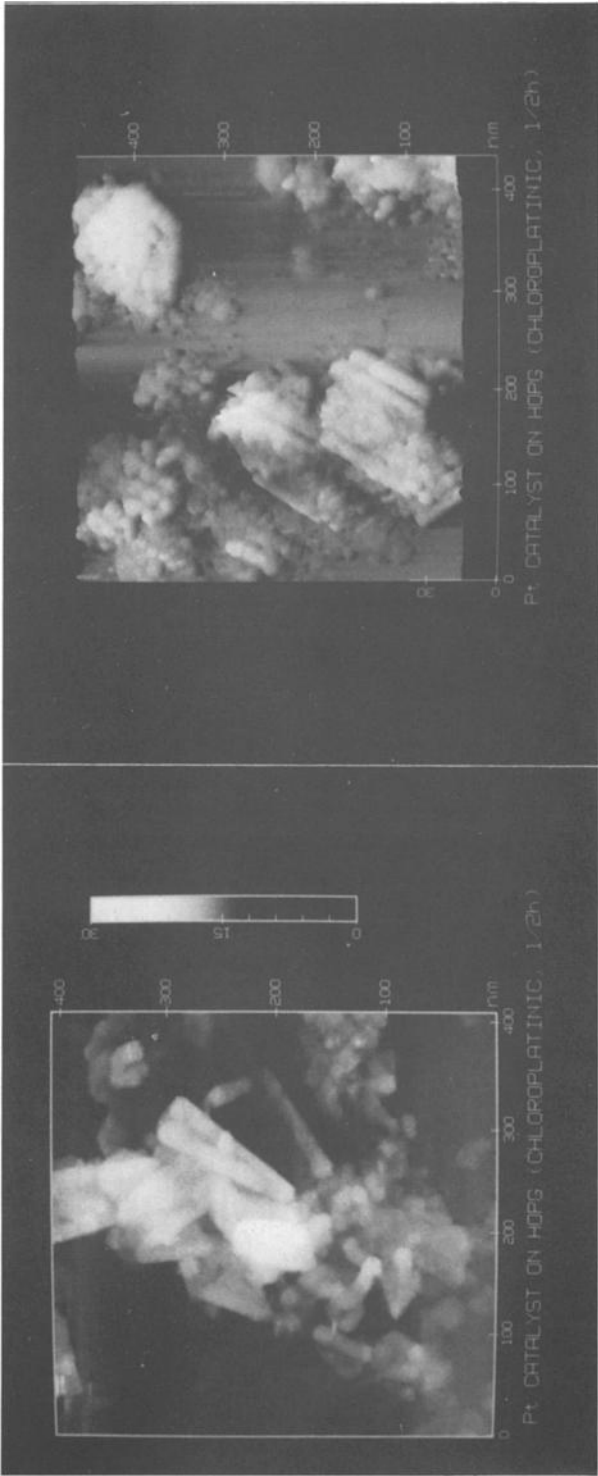


Fig. 1a-b. Pt crystallites (chemical impregnation) after 30 min reduction in H<sub>2</sub>.

breaks up into separate elongated rod-like particles (figs. 1a and 1b), which in turn decompose into smaller and smaller particles (fig. 1b) until the final metallic crystallites are formed.

The large particles are rod-like in shape with length ranging from 100–200 nm and a width between 10–50 nm, whereas the smaller crystallites are oblong in shape with an average size of  $\sim 280$  Å and a height of only  $\sim 30$  Å giving an average particle size of 650 Å for the sample.

*b.) 2.0 hours* Pt particles reduced for 2 hours displayed in fig. 2 show a very different crystallite size and morphology compared to that of the catalyst reduced for 0.5 hours. Although aggregation of the crystallites is still prevalent (fig. 2a), the size and shape of the crystallites are more uniform with random orientation within the aggregates. In this catalyst two types of aggregates were observed; aggregates containing a mixture of both sintered and unsintered particles and that of purely unsintered crystallites. In the unsintered aggregates, the crystallites are loosely bound and can be individually distinguished from one another. The morphology of a single Pt crystallite, shown in fig. 2b, has an ellipsoidal shape with no apparent facets and the height suggests a plate-like morphology similar to that proposed by Winterbottom [21] for supported crystallites. The average size of the crystallites measured from both individual and unsintered aggregates is  $\sim 250$  Å with the height of only  $\sim 20$  Å. The sintered particles are not included in the measurements due to their irregular shapes and difficulty in deciding whether to consider it as a single particle or multiple crystallites.

*c.) 60 hours* After 60 hours of reduction in  $H_2$ , the sizes and geometry of the Pt crystallites undergo a significant change as shown in fig. 3. There is little resemblance between the geometries of the crystallites shown in fig. 3 to either that of the catalyst particles shown in fig. 1 or fig. 2. Although the aggregation of the crystallites is still apparent (fig. 3a), the morphology of the individual crystallites is box-like with well developed facets rather than ellipsoidal. An image at higher magnification image of two individual crystallites (fig. 3b) shows that although the facets are well developed, the surface of the facets is rough and the edges along the perimeter are irregular and kinked. The average size of the crystallites is  $\sim 170$  Å with a height of  $\sim 20$  Å.

A second model Pt catalyst was prepared by vacuum depositing the equivalent of 10 Å thin film of Pt on NGHPG substrates and subsequently treated with  $H_2$  (250°C, 30 min). Images of the resulting crystallites (fig. 4a) show that they are approximately spherical in shape with sizes between 25 to 100 Å. The absence of facets and spherical morphology of the crystallites indicates surface roughness. A higher resolution image (fig. 4b) of the crystallites in fig. 4a shows the atomic structure of the crystallite's surface. However prior to  $H_2$  treatment, the deposited Pt forms irregularly shaped particles which have no resemblance to that obtained from wet impregnation.

The morphological transformation of the Pt crystallites from fig. 1 to fig. 3 is

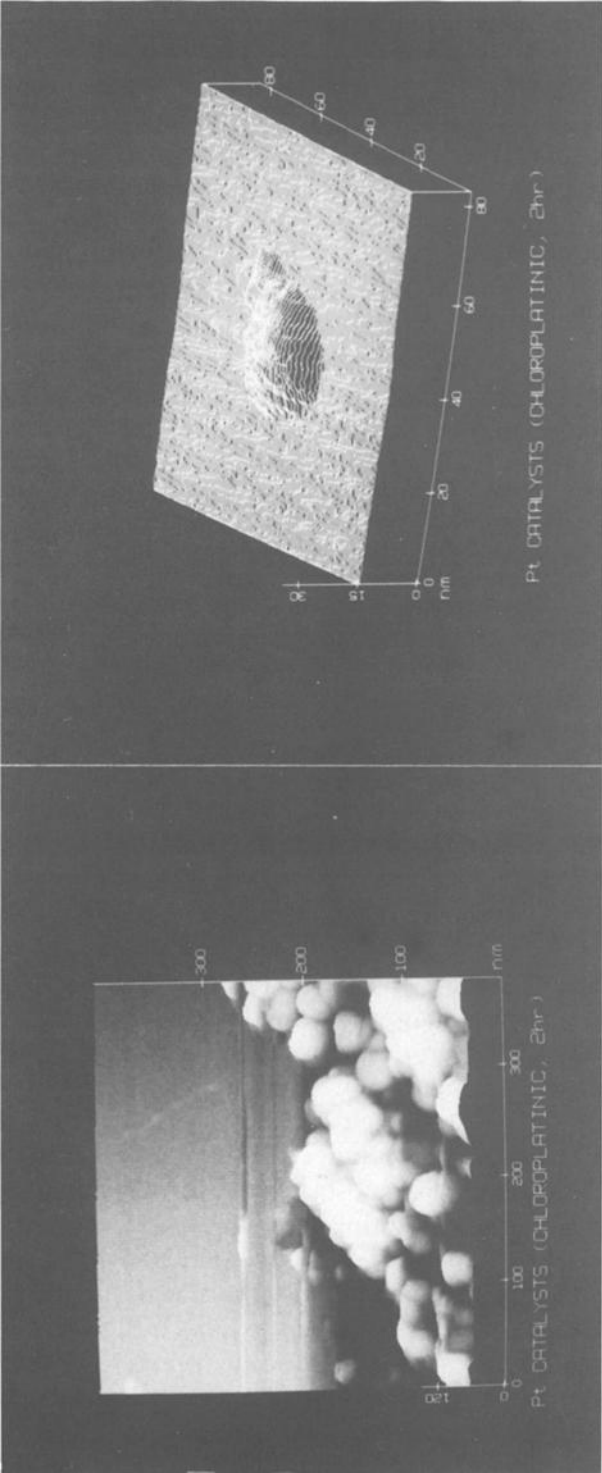


Fig. 2a-b. Pt crystallites (chemical impregnation) after 2 h reduction in H<sub>2</sub>.

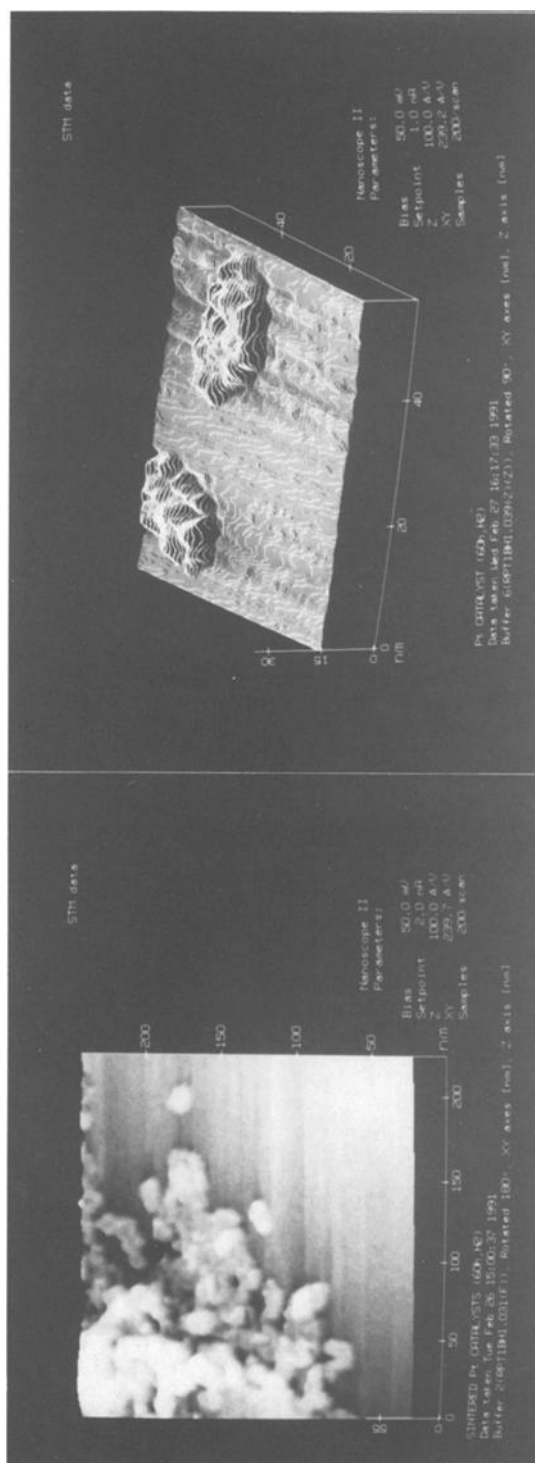


Fig. 3a-b. Pt crystallites (chemical impregnation) after 60 h reduction in  $H_2$ .

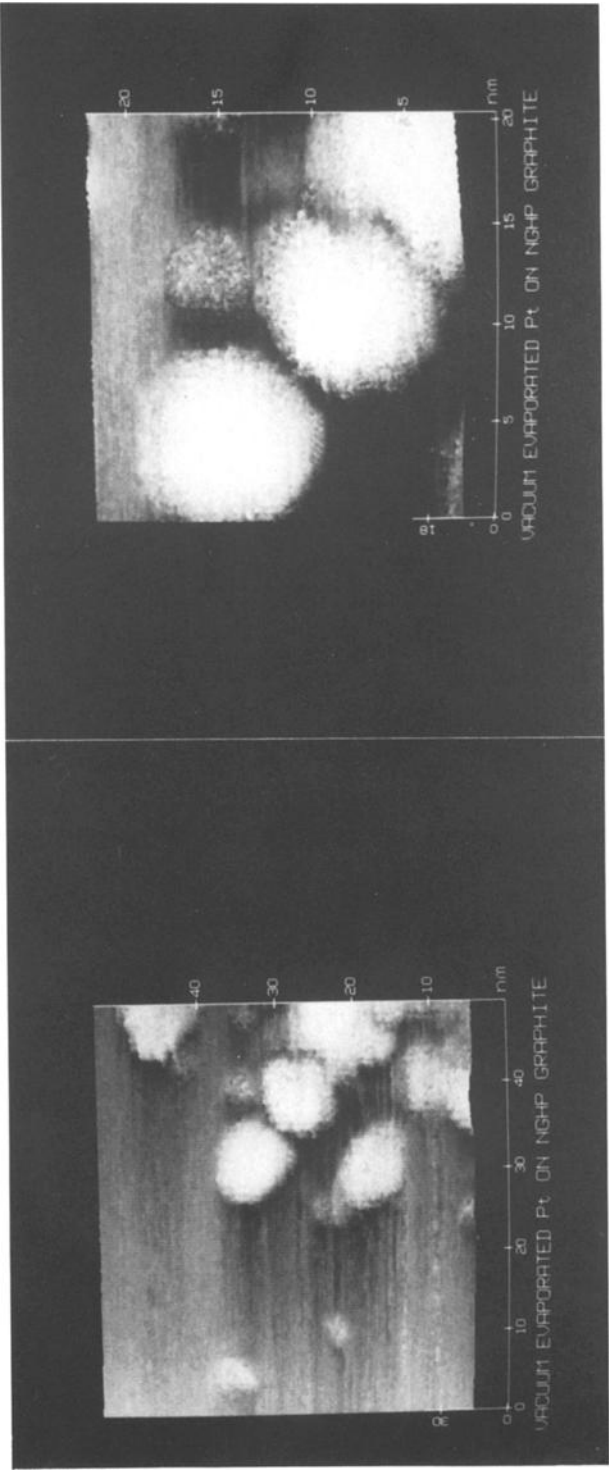


Fig. 4a-b. Pt crystallites (vacuum deposited) after 30 min pretreatment in H<sub>2</sub>.



interesting because it charts the process of transformation from catalyst intermediates to reduced crystallites of near equilibrium morphology. The results suggest that the catalyst intermediates decompose by first breaking into rod-like particles which in turn further decompose into smaller particles. Comparison of the average sizes between the particles in fig. 1 (650 Å) to the crystallites in fig. 2 (250 Å) shows that the particles did decompose further to form the reduced crystallites of ellipsoidal shape. The morphology of these crystallites have close similarity to the model catalyst shown in fig. 4 with the crystallites of the latter being smaller and more spherical in shape. Longer reduction time allows the crystallites to form well developed facets (fig. 3) and approach equilibrium morphology.

All of the supported Pt crystallites exhibit an anomalous height indicating a plate-like morphology similar to the truncated crystallite shape proposed by Winterbottom [21] for crystallites on flat supports. The STM results show a height to length ratio of about 1: 6 as compared to the lower limit of 1:2 from transmission electron microscopy (TEM) studies of metal particles supported on oxide surfaces [22–24]. This height anomaly can be partly attributed to the characteristic of the graphite substrate used in this study compared to the oxide supports used in TEM studies. The presence of the burn-holes near some of the crystallites observed in the study, implies that they may be partially buried within the substrate. Burn-holes are shallow pits created by partial gasification of the graphite substrate during pretreatment of the catalyst which become exposed when the crystallites are displaced from its original location. While the embedment of the crystallites can explain some of the height discrepancy, it is also conceivable that the surfaces of the crystallites are partially covered by surface impurity (carbon or oxygen) which can affect both the chemistry and conductivity of the surface, and tunneling through this layer can create distortion in the measured height.

#### ASPECT RATIO DISTRIBUTION (LTW) OF Pt SUPPORTED CATALYSTS

To quantify physical shapes and morphologies of metal crystallites, elaborate methods have been developed such as geometry fittings [25] and fractal measurements [26]. In this study we will employ the length to width (LTW) ratio or aspect ratio, because it gives a good indication of the crystallite shapes with the least amount of computation time. Fig. 5 shows the aspect ratio distribution of the crystallites in Pt/HOPG catalysts for the reduction times of 0.5, 2.0 and 60.0 hours. The distributions show that the percentage of crystallites with  $LTW = 1.0$  increases monotonically from 27 to 38% with reduction time while the percentage of crystallites with  $LTW = 1.2$  and  $1.4$  reaches maximum at a reduction time of 2 h. The distribution shows a significant increase in the crystallites with equilibrium aspect ratio ( $LTW = 1.0$ ) with reduction time, at the expense of the crystallites with metastable shapes ( $LTW > 1.0$ ) indicating a significant shift in

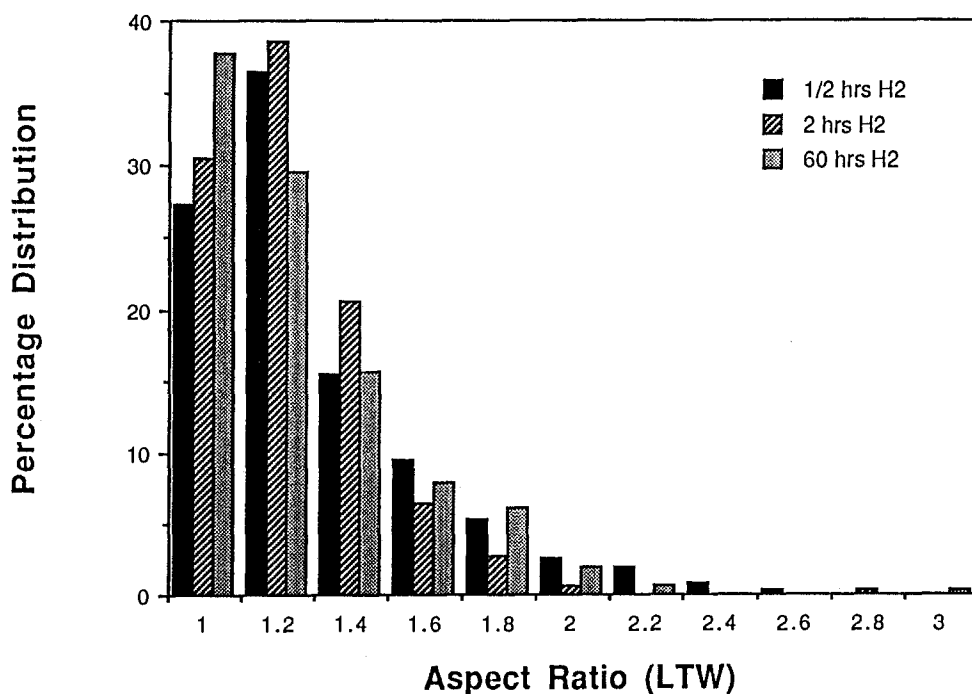


Fig. 5. Aspect ratio (LTW) distribution of Pt crystallites (chemical impregnation) for 30 min, 2 h and 60 h reduction in  $H_2$ .

the crystallite shapes toward equilibrium. The final distribution curve (60 h) assumes an exponential decreasing population as the LTW ratio increases. Aspect ratio distribution for Pt catalysts prepared from tetraamine platinum nitrate (TPN) precursors exchanged onto HOPG (Pt/HOPG T2) and NGHPG (Pt/NGHPG T2) substrates, Pt catalyst from chloroplatinic acid impregnated onto HOPG (Pt/HOPG CA), and Pd catalysts from tetrapyrindine palladium chloride on HOPG (Pd/hopg P2) shown in fig. 6 exhibit similar aspect ratio distribution independent of the precursors and preparation methods used. This shows that the *aspect ratio* distribution of the crystallites is affected mainly by the pretreatment conditions and to a lesser extent by both catalyst precursors, type of graphite supports, and method of preparation.

Crystallites with close value of the aspect ratio such as  $LTW = 1.0$  and  $1.2$  are very difficult to distinguish from one another with other microscopic techniques, and fig. 5 and fig. 6 show that 70% of the crystallites have  $LTW = 1.0$  and  $1.2$  giving a false appearance of uniformity in crystallite shapes. The aspect ratio can be used to gauge the thermodynamic condition of the supported Pt crystallites. Platinum crystallite has a FCC structure and will have an aspect ratio of  $1.0$  at thermodynamic equilibrium. The aspect ratio distributions shown in fig. 5 and fig. 6 show that only  $\sim 30\text{--}40\%$  of the crystallites have  $LTW = 1.0$  while

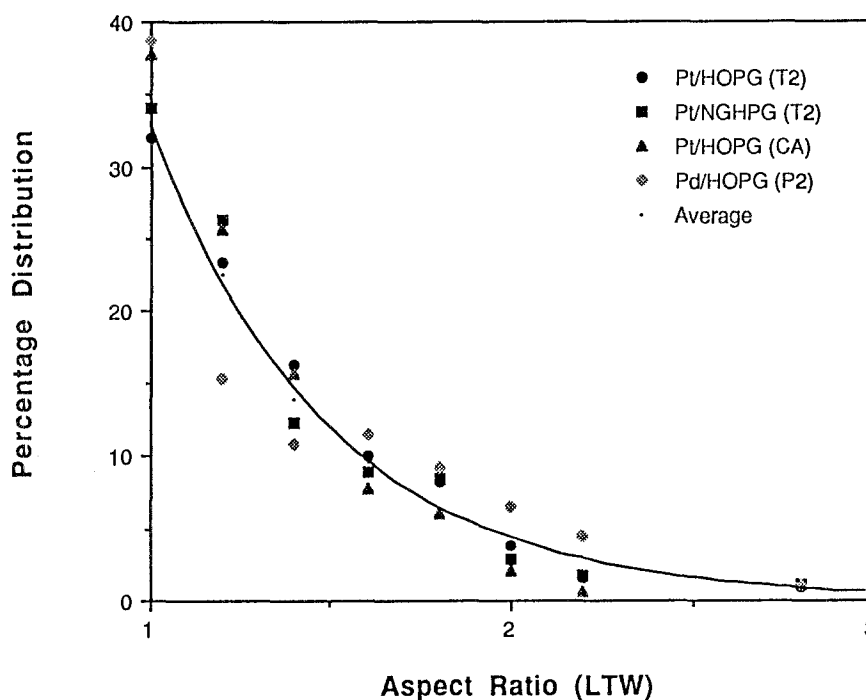


Fig. 6. Aspect ratio (LTW) distribution of Pt and Pd crystallites (chemical impregnation) for different substrates, precursors and preparations.

60–70% have  $LTW > 1.0$  indicating the majority of the crystallites in these catalysts have a metastable morphology.

#### 4. Summary

The effect of  $H_2$  pretreatment of the model Pt catalysts supported on graphite have been investigated. The particles of the model catalysts prepared via chemical impregnation have rod-like morphology at short pretreatment time that appears to be the result of partial reduction of the salt precursor. As the pretreatment progresses, the rod-like particles decomposed to crystallites with ellipsoidal shape and further treatment results in box-like morphology with well developed facets characteristic of FCC metals. The dynamics of morphological transformation of the crystallites with pretreatment time can be clearly seen from the aspect ratio (LTW) distributions which shows a displacement of the population with LTW values larger than 1.0 toward 1.0 as the pretreatment time increases. This shows that as pretreatment time increases, the crystallites with elongated shape ( $LTW > 1.0$ ) diminishes. The distribution of the crystallites shape is affected mainly by the pretreatment condition and to a lesser extent by the catalyst precursor, type of graphite support and method of preparation. Pt

catalyst prepared from vacuum evaporation of Pt metals onto a graphite support exhibits irregular but reproducible particles prior to H<sub>2</sub> pretreatment. After H<sub>2</sub> pretreatment (250°C) for 30 min, the initially large, irregularly shaped particles transform into spherical crystallites of 25–100 Å sizes. The higher resolution STM images of spherical crystallites show the surface atomic structure to be that of rough surface. The results obtained demonstrate that STM is capable of providing both morphological and structural information of rough particles and that H<sub>2</sub> treatment is an important factor shaping these Pt supported catalysts.

### Acknowledgements

Funds to purchase the equipment were provided by NSF CBT 88-06640 and the research was funded by NSF CTS 90-01586.

### References

- [1] G. Binnig, H. Rohrer, Ch. Gerber and E. Weibel, *Phys. Rev. Lett.* 50 (1983) 120.
- [2] A. Baratoff, G. Binnig, H. Fuchs, F. Salvan and E. Stoll, *Surf. Sci.* 168 (1986) 734.
- [3] R.J. Hamers and J.E. Demuth, *Phys. Rev. Lett.* 60 (1988) 2527.
- [4] Y. Kuk, P.J. Silverman and F.M. Chua, *J. of Microscopy* 152 (1988) 449.
- [5] Y. Kuk and P.J. Silverman, *J. Vac. Sci. Technol. A* 8 (1990) 289.
- [6] S. Rousset, S. Gauthier, O. Siboulet, W. Sacks, M. Belin and J. Klein, *J. Vac. Sci. Technol. A* 8 (1990) 302.
- [7] F.M. Chua, Y. Kuk and P.J. Silverman, *J. Vac. Sci. Technol. A* 8 (1990) 305.
- [8] R.J. Behm, W. Hosler, E. Ritter and G. Binnig, *Phys. Rev. Lett.* 56 (1986) 228.
- [9] L. Vazquez, J.M. Gomez Rodriguez, J. Gomez Herrero, A.M. Baro, N. Garcia, J.C. Canullo and A.J. Arvia, *Surf. Sci.* 181 (1987) 98.
- [10] J. Wintterlin, J. Wiechers, H. Brune, T. Gritsch, H. Hofer and R.J. Behm, *Phys. Rev. Lett.* 62 (1989) 59.
- [11] R. Nishitani, A. Kasuya, S. Kubota and Y. Nishina, *J. Vac. Sci. Technol. B* 9 (1991) 806.
- [12] A. Humbert, M. Dayez, S. Granjeaud, P. Ricci, C. Chapon and C.R. Henry, *J. Vac. Sci. Technol. B* 9 (1991) 802.
- [13] R. Moffat Kennedy, X. Yang and D. Fennel Evans, *J. Vac. Sci. Technol. B* 9 (1991) 735.
- [14] C. Becker, Th. Fries, K. Wandelt, U. Kreibig and G. Schmid, *J. Vac. Sci. Technol. B* 9 (1991) 810.
- [15] A.M. Baro, A. Bartolome, L. Vazquez, N. Garcia, R. Reifenberger, E. Choi and R.P. Andres, *Appl. Phys. Lett.* 51 (1987) 1594.
- [16] M. Komiyama, S. Morita and N. Mikoshiba, *J. Microscopy* 152 (1988) 197.
- [17] M. Komiyama, J. Kobayashi and S. Morita, *J. Vac. Sci. Technol. A* 8 (1990) 608.
- [18] King Lun Yeung and E.E. Wolf, *J. Vac. Sci. Technol. B* 9 (1991) 798.
- [19] J. Colchero, O. Marti, J. Mlynek, A. Humbert, C.R. Henry and C. Chapon, *J. Vac. Sci. Technol. B* 9 (1991) 794.
- [20] U. Muller, K. Satter, J. Xhie, N. Venkateswaran and G. Raina, *J. Vac. Sci. Technol. B* 9 (1991) 829.
- [21] W.L. Winterbottom, *Acta Metall.* 15 (1967) 303.

- [22] A.K. Datye, A.D. Logan and N.J. Long, *J. Catal.* 109 (1988) 76.
- [23] S. Chakraborti, A.K. Datye and N.J. Long, *J. Catal.* 108 (1987) 444.
- [24] J.C. Heyraud and J.J. Metois, *J. Crystal Growth* 50 (1980) 571.
- [25] T.G. Smith, Jr., W.B. Marks, G.D. Lange, W.H. Sheriff Jr. and E.A. Neale, *J. Neurosci. Methods* 27 (1989) 173.
- [26] D. Avnir, *The Fractal Approach to Heterogeneous Chemistry; Surfaces; Colloids, Polymers* (John Wiley & Sons, New York, 1989).